Fluorescent Probes

Deutsche Ausgabe: DOI: 10.1002/ange.201510003
Internationale Ausgabe: DOI: 10.1002/anie.201510003

A Multisite-Binding Switchable Fluorescent Probe for Monitoring Mitochondrial ATP Level Fluctuation in Live Cells

Lu Wang, Lin Yuan, Xian Zeng, Juanjuan Peng, Yong Ni, Jun Cheng Er, Wang Xu, Bikram Keshari Agrawalla, Dongdong Su, Beomsue Kim, and Young-Tae Chang**

Abstract: *Adenosine triphosphate (ATP), commonly produced in mitochondria, is required by almost all the living organisms; thus fluorescent probes for monitoring mitochondrial ATP levels fluctuation are essential and highly desired. Herein, we report a multisite-binding switchable fluorescent probe, ATP-Red* ***1****, which selectively and rapidly responds to intracellular concentrations of ATP. Live-cell imaging indicated that ATP-Red* ***1*** *mainly localized to mitochondria with good biocompatibility and membrane penetration. In particular, with the help of ATP-Red* ***1****, we successfully observed not only the decreased mitochondrial ATP levels in the presence of KCN and starvation state, but also the increased mitochondrial ATP levels in the early stage of cell apoptosis. These results indicate that ATP-Red* ***1*** *is a useful tool for investigating ATP-relevant biological processes.*

Adenosine triphosphate (ATP), an indispensable biomolecule, is shared by almost all independently living organisms on Earth. As the molecular unit of currency, ATP is the primary energy source for cellular processes.[1] ATP also functions as a signaling molecule for regulating cell movement,[2] neurotransmission,[3] and ion channels.[4] In mitochondria, ATP is recharged by the addition of phosphate to adenosine diphosphate (ADP) through oxidative phosphorylation (OXPHOS). Thus, mitochondrial ATP plays a central role in regulating the cellular energy status for metabolic activities in healthy and diseased states.[5] Therefore, there is a compelling need for molecular probes to track and image mitochondrial ATP and further elucidate its contributions to physiological states.

Several off-line analytic methods have been applied to measure ATP concentration of cell extracts.[6] Compared with these methods, fluorescence imaging shows specific advantages in the research of functional- and molecular-recognition events in live cells.[7] Recently, several genetically encoded or aptamer-based fluorescent ATP probes have been developed and applied in live-cell imaging.[8] However, small-molecule probes show complementary properties, such as ease of operation and low cost. Thus, some small-molecule fluorescent ATP probes, mainly based on complexation with imidazolium[9] or metal ions,[10] have been developed. However, owing to the challenges in overcoming issues of selectivity and response concentration, only a few ATP sensors have been applied for cell imaging.[9,10c,e,l] In particular, fewer probes are suitable to monitor the increased ATP levels because of the narrow response range and low saturation concentration.[10l] At the same time, despite the essential roles of mitochondrial ATP, only two recent fluorescent probes were successfully used for mitochondrial ATP imaging.[10c,l] Thus, preparing a good sensor for monitoring the fluctuation of mitochondrial ATP levels remains a challenge.

The current design strategy for sensing ATP is mainly based on the electrostatic interaction between negatively charged phosphates of ATP and positively charged recognition groups, such as imidazolium and metal ions. However, in most cases, the stability and selectivity of these probes were not satisfying owing to the interference from nucleoside polyphosphates (NPPs) or negatively charged biomolecules. To tackle these problems, herein, a multisite-binding strategy was applied. Considering the three main parts of NPPs (vicinal diol, nitrogenous base, and phosphates; Figure 1 A), we envisioned that covalent bonding, π-π interactions, and electronic attraction could cooperate to achieve the specific recognition of ATP. It has been reported that phenylboronic acid can reversibly react with diols, and such motifs have been applied to detect carbohydrates inside cells.[11] Therefore, a phenylboronic acid was introduced into Rhodamine B linked at *ortho*-, *meta*-, and *para*-positions, respectively, to obtain ATP-Red **1**–**3** (Supporting Information, Scheme S1). It was hypothesized that these probes would be non-fluorescent when forming a ring-closed structure; in the presence of ATP, however, a covalent bond between boronic acid and ribose, π-π interaction between xanthene and adenine, and electrostatic interactions between amino and phosphate groups function cooperatively to facilitate the ring-opening structure of the probe, thereby generating strong

[*] L. Wang, Prof. Dr. L. Yuan, J. C. Er, W. Xu, B. K. Agrawalla, Prof. Dr. Y.-T. Chang
Department of Chemistry and Medicinal Chemistry Programme
National University of Singapore
Singapore 117543 (Singapore)
E-mail: chmcyt@nus.edu.sg
Prof. Dr. L. Yuan
State Key Laboratory of Chemo/Biosensing and Chemometrics
College of Chemistry and Chemical Engineering
Hunan University
Changsha 410082 (PR China)
E-mail: lyuan@hnu.edu.cn
X. Zeng
Department of Pharmacy
National University of Singapore
Singapore 117543 (Singapore)
Dr. J. Peng, Dr. Y. Ni, Dr. D. Su, Dr. B. Kim, Prof. Dr. Y.-T. Chang
Laboratory of Bioimaging Probe Development
Singapore Bioimaging Consortium
Singapore 138667 (Singapore)

Supporting information and ORCID(s) from the author(s) for this article are available on the WWW under http://dx.doi.org/10.1002/anie.201510003.

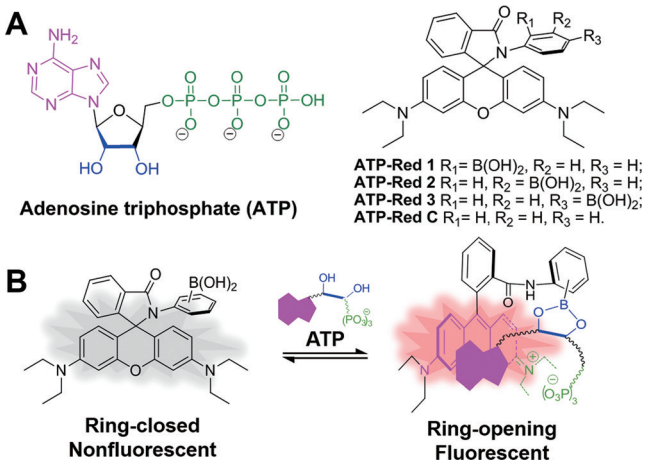

Figure 1. A) Structures of ATP and ATP probes. B) Proposed mechanism for sensing ATP.

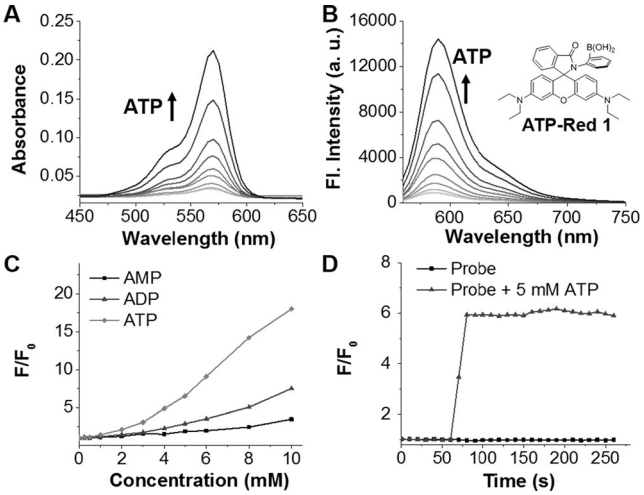

Figure 2. UV absorption (A) and fluorescence (B) spectra of ATP-Red **1** (10 μM) responding to ATP at intracellular concentrations (0–10 mM). C) Fluorescence titration curve of ATP-Red **1** upon the addition of ATP (blue), ADP (red) and AMP (black). [Analytes] = 0–10 mM. D) Time-dependence of the fluorescence intensity change before and after treatment of ATP. [ATP] = 5 mM. Time interval: 10 s. F/F_0 represents the fluorescence intensity ratio (590 nm) and F_0 is the initial fluorescence intensity (590 nm) of ATP-Red **1** in the absence of nucleoside polyphosphates. Conditions: λ_{ex}: 510 nm, [ATP-Red **1**] = 10 μM, Glycerol/Krebs buffer solution (60/40, pH 7.8), 25 °C.

fluorescence (Figure 1B; Supporting Information, Table S1). ATP-Red **1**–**3** and a control probe ATP-Red **C** were prepared and characterized by ^{1}H NMR, ^{13}C NMR, and high resolution mass spectrometry (Supporting Information).

Initially, the fluorescence response of ATP-Red **1**–**3** (10 μM) toward ATP were evaluated in buffered (Krebs, pH 7.8) water/glycerol (40:60, v/v) solution, which mimics mitochondrial pH and viscosity.[12] As shown in Figure S1, ATP-Red **1** displayed the strongest fluorescence response to ATP. This may be because the larger steric hindrance of phenylboronic acid at *ortho* position is favorable for the fluorescent ring-opening structure in the presence of ATP. Thus, ATP-Red **1** was chosen as an ATP sensor and tested in the subsequent experiments.

Absorption and fluorescence spectra of ATP-Red **1** were recorded with titration of ATP from 0.5 to 10 mM, a range that is comparable to intracellular ATP concentrations.[13a] An increased absorption band at $\lambda = 570$ nm was observed upon the addition of ATP (Figure 2A), which supports the assumption of the ring-opening process. A solution of 10 μM ATP-Red **1** was weakly fluorescent, while addition of 10 mM ATP led to an 18.1-fold turn-on response (Figure 2B). Similar fluorescence enhancements were also observed not only in buffer solution containing high concentration of carbohydrates (Figure S2), but also in buffer solution mimicking intracellular protein and ion concentrations (Figure S3). ADP and AMP (adenosine monophosphate), partially dephosphorylated products of ATP, are persistent sources of interference in ATP detection. Thus, the fluorescence intensity of ATP-Red **1** was tested by titrating with ADP and AMP, which showed qualitatively similar, but much smaller changes in the spectra (Figure 2C; Supporting Information, Figure S4). The corresponding dissociation constant (K_d) of ATP-Red **1** with ATP, ADP, and AMP were shown in Figure S5. Importantly, the fluorescence response of ATP-Red **1** was also obtained in the buffer solution with different ATP/ADP ratios (Figure S6). Except for the spectral signatures, the sensing process could be achieved within 20 seconds, thus enabling monitoring of intracellular ATP (Figure 2D). Furthermore, pH titration experiments indicated the response capability of ATP-Red **1** to ATP at physiological pH (5.5–7.8; Figure S7).

The selectivity evaluation of ATP-Red **1** toward ATP against various biomolecules was performed. The fluorescence intensity of ATP-Red **1** increased 5.6-fold in the presence of 5 mM ATP (Figure 3), while no significant increase in fluorescence was observed after addition of other biomolecules, such as metal ions and carbohydrates (entries 1–20). Notably, NPPs, which easily compete with ATP detection, only caused slight fluorescence intensity increase in this work (Figure 3, entries 21–32). Moreover, it

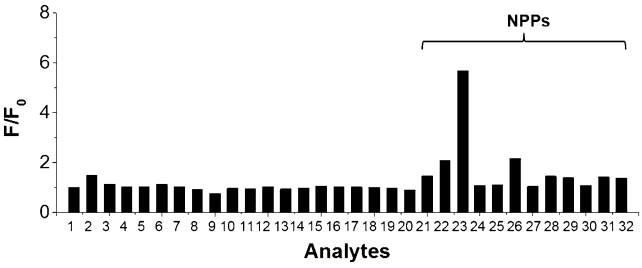

Figure 3. A) Fluorescence response of ATP-Red **1** to various biomolecules. Analytes (5 mM): 1) buffer, 2) Zn^{2+}, 3) Mg^{2+}, 4) Ca^{2+}, 5) Na^+, 6) K^+, 7) GSH, 8) HOCl, 9) H_2O_2, 10) D-arabinose, 11) L-arabinose, 12) D-galactose, 13) D-glucose, 14) D-fructose, 15) D-ribose, 16) L-ribose, 17) L-sorbose, 18) sucrose, 19) D-xylose, 20) heparin, 21) AMP, 22) ADP, 23) ATP, 24) CMP, 25) CDP, 26) CTP, 27) UMP, 28) UDP, 29) UTP, 30) GMP, 31) GDP, 32) GTP. F/F_0 represents the fluorescence intensity ratio (590 nm) and F_0 is the initial fluorescence intensity (590 nm) of ATP-Red **1** in the absence of biomolecules. Conditions: [ATP-Red **1**] = 10 μM, Glycerol/Krebs buffer solution (60/40, pH 7.8). λ_{ex}: 510 nm, 25 °C.

was reported that intracellular ATP is two-fold higher in concentration than UTP and GTP, and more than five-fold higher than other NPPs.[13] Under these conditions, ATP-Red **1** showed excellent selectivity for ATP over other NPPs (Figure S8), indicating that ATP-Red **1** is a promising fluorescent probe for detecting intracellular ATP.

To demonstrate the function of the covalent bond the in multisite binding process, control probe ATP-Red **C** without boronic acid was synthesized.[14] The fluorescence of ATP-Red **C** remained weak in the presence of ATP (Figure S9). The proposed covalent bond between boronic acid and diol of ATP was further demonstrated by MALDI-TOF mass spectrometry (Figure S10). We assumed that π-π stacking between xanthene and adenine is stronger than other nitrogenous bases, which would benefit the recognition of adenosine polyphosphates. Furthermore, the positively charged amino group of the probe forms stronger electrostatic interactions with the negatively charged phosphate anions of ATP than that of ADP and AMP, because ATP has more negative charges at physiological pH. In particular, the proposed multisite-binding was demonstrated by theoretical calculations (Figure S11). The reversibility of the sensing process was indicated by addition of apyrase, which catalyzes the hydrolysis of ATP to yield AMP. As shown in Figure S12, after ATP consumption, the fluorescence intensity decreased significantly owing to the recovery of the non-fluorescent ring-closed structure.

To evaluate the biocompatibility of ATP-Red **1**, an MTT assay was performed and indicated no significant effects on cell viability at the concentration of 1–8 μM after incubation for 3 h or 24 h (Figure S13). Intracellular distribution of ATP-Red **1** was examined in oral squamous cell carcinoma (OSCC) cells (Figure 4) and HeLa cells (Figure S14). The strong fluorescence signal of ATP-Red **1** colocalized well with that of Mito-Tracker Green in mitochondria (Pearson's Coefficient: 0.894) but not that of Lyso-Tracker Green in lysosome, or Hoechst in nucleus. The specific mitochondrial distribution may result from the cooperatively function of the negative

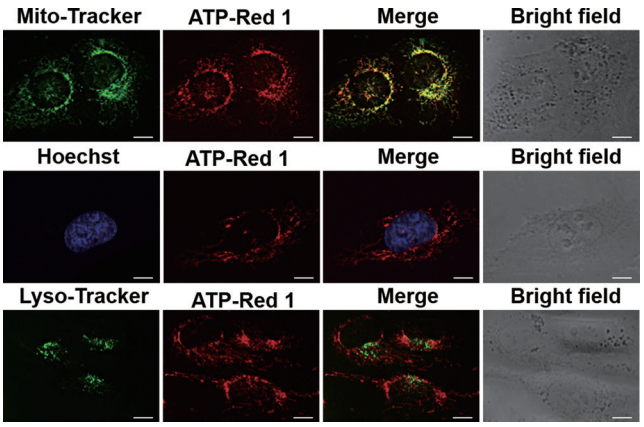

Figure 4. Intracellular localization of ATP-Red **1** in OSCC cells. Live OSCC cells were prestained with ATP-Red **1** (5 μM, 15 min) and further treated with Mito-Tracker Green (0.25 μM, 15 min), Lyso-Tracker Green (1 μM, 60 min), or Hoechst (1 μM, 15 min), respectively. Yellow: merged signal. Green: MitoGreen and LysoGreen; blue: Hoechst; red: ATP-Red **1**. Scale bar: 10 μm.

mitochondrial membrane potential,[15] high viscosity, and ATP concentration in mitochondria (Figure S15). The cell experiment also indicated good membrane permeability of ATP-Red **1**, which would benefit live-cell imaging.

We therefore examined the applicability of ATP-Red **1** to monitor mitochondrial ATP levels in living cells. As shown in Figure 5Aa, OSCC cells incubated with 5 μM ATP-Red **1**

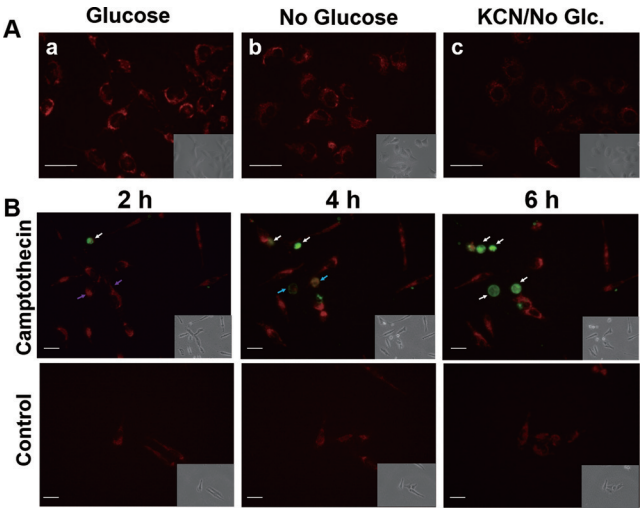

Figure 5. A) Fluorescence images of ATP-Red-**1** (5 μM, 20 min)-stained live OSCC cells in the presence/absence of KCN (0.5 mM, 0.5 h) and starvation conditions. B) Fluorescence images of ATP-Red **1** (2.5 μM, 20 min)-stained live OSCC cells incubated with/without camptothecin (10 μM) for 2, 4, and 6 h, respectively. Green: Annexin V (cell apoptosis tracker); red: ATP-Red **1**. Arrows indicate the cell apoptosis process. Scale bar: 30 μm.

presented strong fluorescence in the red channel. To verify that the fluorescence was induced by mitochondrial ATP, glucose, the precursor for the synthesis of ATP, was removed from the medium.[8c] As expected, a slight fluorescence decrease was observed (Figure 5Ab; Supporting Information, Figure S16). OSCC cells were further incubated with KCN, an inhibitor of OXPHOS, under glucose starvation conditions.[10f,16] Subsequent ATP-Red **1** staining showed much weaker fluorescence (Figure 5Ac; Supporting Information, Figure S16), indicating the significantly reduced mitochondrial ATP levels after KCN-induced inhibition of OXPHOS. A similar effect was also observed in live HeLa cells (Figure S17).

To demonstrate the capability of ATP-Red **1** to monitor increased ATP levels, camptothecin was used to induce cell apoptosis because elevation of intracellular ATP levels is a requisite to the apoptotic cell death process.[17] Time lapse imaging displayed that OSCC cells incubated with camptothecin showed much stronger fluorescence (red), which indicates higher ATP concentration in mitochondria during apoptosis process (Figure 5B and S18). This conclusion was also demonstrated by flow cytometry analysis (Figure S19). To confirm the apoptotic process, Annexin V, a cell apoptosis tracker, was administered. No signal from Annexin V was observed in the untreated control group, while camptothecin-

treated cells were clearly stained (Figure 5B; Supporting Information). Even though increased cytosolic ATP levels is required during apoptosis, the origin of the increased ATP, whether from cytosolic glycolysis or mitochondrial OXPHOS, remains unclear.[17a,18] The above results gave rise to indications that elevated mitochondrial ATP levels may contribute to the elevation of cytosolic ATP during cell apoptosis.

In conclusion, a multisite-binding, switchable fluorescent probe, ATP-Red **1**, was successfully developed and applied to sense ATP in living cells. On account of the multisite-binding strategy, ATP-Red **1** could selectively and rapidly respond to ATP at intracellular concentrations. ATP-Red **1** was found to mainly localize to mitochondria, with good biocompatibility and membrane penetration. Significantly, ATP-Red **1** was successfully applied to monitor both increased and decreased mitochondrial ATP levels. This ATP sensor not only works as an excellent fluorescent indicator for detecting mitochondrial ATP, but also provides a practical and efficient strategy to design the NPPs probes.

Acknowledgements

This work was supported by intramural funding from A*STAR (Agency for Science, Technology and Research, Singapore), Biomedical Research Council, and National Medical Research Council grant (NMRC/CBRG/0015/2012).

Keywords: ATP · cell imaging · fluorescent probes · multisite-binding

How to cite: *Angew. Chem. Int. Ed.* **2016**, *55*, 1773–1776
Angew. Chem. **2016**, *128*, 1805–1808

[1] a) J. R. Knowles, *Annu. Rev. Biochem.* **1980**, *49*, 877–919; b) C. F. Higgins, I. D. Hiles, G. P. Salmond, D. R. Gill, J. A. Downie, I. J. Evans, I. B. Holland, L. Gray, S. D. Buckel, A. W. Bell, et al., *Nature* **1986**, *323*, 448–450.

[2] D. Davalos, J. Grutzendler, G. Yang, J. V. Kim, Y. Zuo, S. Jung, D. R. Littman, M. L. Dustin, W. B. Gan, *Nat. Neurosci.* **2005**, *8*, 752–758.

[3] G. Burnstock, *Trends Pharmacol. Sci.* **2006**, *27*, 166–176.

[4] F. M. Ashcroft, F. M. Gribble, *Diabetologia* **1999**, *42*, 903–919.

[5] a) M. T. Lin, M. F. Beal, *Nature* **2006**, *443*, 787–795; b) D. G. Hardie, F. A. Ross, S. A. Hawley, *Nat. Rev. Mol. Cell Biol.* **2012**, *13*, 251–262.

[6] a) G. Manfredi, L. Yang, C. D. Gajewski, M. Mattiazzi, *Methods* **2002**, *26*, 317–326; b) M. Li, J. Zhang, S. Suri, L. J. Sooter, D. Ma, N. Wu, *Anal. Chem.* **2012**, *84*, 2837–2842; c) E. Gout, F. Rebeille, R. Douce, R. Bligny, *Proc. Natl. Acad. Sci. USA* **2014**, *111*, E4560–E4567.

[7] a) V. S. Lin, W. Chen, M. Xian, C. J. Chang, *Chem. Soc. Rev.* **2014**, *43*, 3183; b) H. Kobayashi, M. Ogawa, R. Alford, P. L. Choyke, Y. Urano, *Chem. Rev.* **2010**, *110*, 2620–2640; c) J. W. Lichtman, J. A. Conchello, *Nat. Methods* **2005**, *2*, 910–919; d) A. R. Lippert, G. C. Van de Bittner, C. J. Chang, *Acc. Chem. Res.* **2011**, *44*, 793–804.

[8] a) H. Imamura, K. P. Nhat, H. Togawa, K. Saito, R. Iino, Y. Kato-Yamada, T. Nagai, H. Noji, *Proc. Natl. Acad. Sci. USA* **2009**, *106*, 15651–15656; b) H. Kioka, H. Kato, M. Fujikawa, O. Tsukamoto, T. Suzuki, H. Imamura, A. Nakano, S. Higo, S. Yamazaki, T. Matsuzaki, K. Takafuji, H. Asanuma, M. Asakura, T. Minamino, Y. Shintani, M. Yoshida, H. Noji, M. Kitakaze, I. Komuro, Y. Asano, S. Takashima, *Proc. Natl. Acad. Sci. USA* **2014**, *111*, 273–278; c) A. I. Tarasov, G. A. Rutter, *Methods Enzymol.* **2014**, *542*, 289–311; d) J. Berg, Y. P. Hung, G. Yellen, *Nat. Methods* **2009**, *6*, 161–166; e) T. Morii, M. Hagihara, S. I. Sato, K. Makino, *J. Am. Chem. Soc.* **2002**, *124*, 4617–4622; f) P. Yu, X. L. He, L. Zhang, L. Q. Mao, *Anal. Chem.* **2015**, *87*, 1373–1380.

[9] a) X. Y. Li, X. D. Guo, L. X. Cao, Z. Q. Xun, S. Q. Wang, S. Y. Li, Y. Li, G. Q. Yang, *Angew. Chem. Int. Ed.* **2014**, *53*, 7809–7813; *Angew. Chem.* **2014**, *126*, 7943–7947; b) Z. Xu, N. J. Singh, J. Lim, J. Pan, H. N. Kim, S. Park, K. S. Kim, J. Yoon, *J. Am. Chem. Soc.* **2009**, *131*, 15528–15533.

[10] a) X. Liu, J. Xu, Y. Y. Lv, W. Y. Wu, W. S. Liu, Y. Tang, *Dalton Trans.* **2013**, *42*, 9840–9846; b) E. A. Weitz, J. Y. Chang, A. H. Rosenfield, E. A. Morrow, V. C. Pierre, *Chem. Sci.* **2013**, *4*, 4052–4060; c) P. Srivastava, S. S. Razi, R. Ali, S. Srivastav, S. Patnaik, S. Srikrishna, A. Misra, *Biosens. Bioelectron.* **2015**, *69C*, 179–185; d) A. J. Moro, P. J. Cywinski, S. Korsten, G. J. Mohr, *Chem. Commun.* **2010**, *46*, 1085–1087; e) Y. Kurishita, T. Kohira, A. Ojida, I. Hamachi, *J. Am. Chem. Soc.* **2010**, *132*, 13290–13299; f) A. S. Rao, D. Kim, H. Nam, H. Jo, K. H. Kim, C. Ban, K. H. Ahn, *Chem. Commun.* **2012**, *48*, 3206–3208; g) A. Ojida, I. Takashima, T. Kohira, H. Nonaka, I. Hamachi, *J. Am. Chem. Soc.* **2008**, *130*, 12095–12101; h) E. A. Weitz, J. Y. Chang, A. H. Rosenfield, V. C. Pierre, *J. Am. Chem. Soc.* **2012**, *134*, 16099–16102; i) M. Schäferling, O. S. Wolfbeis, *Chem. Eur. J.* **2007**, *13*, 4342–4349; j) P. Mahato, A. Ghosh, S. K. Mishra, A. Shrivastav, S. Mishra, A, Das, *Chem. Commun.* **2010**, *46*, 9134–9136; k) S. Mameri, L. J. Charnonnière, R. F. Ziessel, *Inorg. Chem.* **2004**, *43*, 1819–1821; l) Y. Kurishita, T. Kohira, A. Ojida, I. Hamachi, *J. Am. Chem. Soc.* **2012**, *134*, 18779–18789.

[11] X. Sun, T. D. James, *Chem. Rev.* **2015**, *115*, 8001–8037.

[12] a) N. Jiang, J. Fan, S. Zhang, T. Wu, J. Wang, P. Gao, J. Qu, F. Zhou, X. Peng, *Sens. Actuators B* **2014**, *190*, 685–693; b) M. H. Lee, N. Park, C. Yi, J. H. Han, J. H. Hong, K. P. Kim, D. H. Kang, J. L. Sessler, C. Kang, J. S. Kim, *J. Am. Chem. Soc.* **2014**, *136*, 14136–14142.

[13] a) M. H. Buckstein, J. He, H. Rubin, *J. Bacteriol.* **2008**, *190*, 718–726; b) I. Allue, O. Gandelman, E. Dementieva, N. Ugarova, P. Cobbold, *Biochem. J.* **1996**, *319*, 463–469.

[14] X. Zhang, Y. Shiraishi, T. Hirai, *Tetrahedron Lett.* **2007**, *48*, 5455–5459.

[15] P. Reungpatthanaphong, S. Dechsupa, J. Meesungnoen, C. Loetchutinat, S. Mankhetkorn, *J. Biochem. Biophys. Methods* **2003**, *25*, 1–16.

[16] Y. Nishimura, L. H. Romer, J. J. Lemasters, *Hepatology* **1998**, *27*, 1039–1049.

[17] a) M. V. Zamaraeva, R. Z. Sabirov, E. Maeno, Y. Ando-Akatsuka, S. V. Bessonova, Y. Okada, *Cell Death Differ.* **2005**, *12*, 1390–1397; b) E. J. Morris, H. M. Geller, *J. Cell Biol.* **1996**, *134*, 757–770.

[18] M. Leist, B. Single, A. F. Castoldi, S. Kuhnle, P. Nicotera, *J. Exp. Med.* **1997**, *185*, 1481–1486.

Received: October 26, 2015
Revised: November 25, 2015
Published online: December 16, 2015

